Analyzing Rear-End Collision Risk Relevant to Autonomous Vehicles by Using a Humanlike Brake Model

Ci Liang, Mohamed Ghazel, Yusheng Ci, Wei Zheng

Analysing rear-end collision risk relevant to autonomous vehicles by using a human-like brake model

Ci Liang[1], Mohamed Ghazel[2], Yusheng Ci[3], and Wei Zheng[4]

[1]Associate Professor, Ph.D., School of Transportation Science and Engineering, Harbin Institute of Technology, CN, 150001. Email: ciliang.lc@gmail.com

[2]Research Director, Ph.D., Université Gustave Eiffel COSYS/ESTAS (ex-IFSTTAR), Campus de Lille, FR, 100044. Email: mohamed.ghazel@univ-eiffel.fr

[3]Associate Professor, Ph.D., School of Transportation Science and Engineering, Harbin Institute of Technology, CN, 150001 (corresponding author). Email: ciyusheng@hit.edu.cn

[4]Professor, Ph.D., Collaborative Innovation Center of Railway Traffic Safety, and School of Automation and Intelligence, Beijing Jiaotong University, CN, 100044. Email: wzheng1@bjtu.edu.cn

ABSTRACT

Rear-end collisions between autonomous vehicles (AVs) and human-driven vehicles (HVs) represent critical scenarios in road networks. Few studies have focused on the scenarios where an HV hits an AV from behind (called HV-AV collision). This paper aims to investigate the occurrence of HV-AV collisions in the Stop-in-Lane (SiL) scenario where an HV follows an AV. A human-like brake control (HLBC) model is firstly proposed to simulate the driver brake control. The HLBC model considers human driving intention, vision-based expectancy and certain inherent characteristics of human driving to achieve dynamic human-like braking. Additionally, the joint distribution of Off-Road-Glance and Time-Headway is originally introduced to simulate the glance distraction of drivers during their dynamic vehicle control. Sequentially, we apply the HLBC model to the SiL scenario to investigate how the HV-AV collision probability changes with respect

to various dynamic driving parameters. The results of the case study provide us a thorough understanding of the dynamic driving conditions that lead to HV-AV collisions, and pave the way for identifying practical countermeasures to improve the road safety involving AVs.

INTRODUCTION

Nowadays, the automotive industry is making a quantum leap toward the future. Road safety involving autonomous driving (AD) is a hot topic for both industry and academia. As we know, a growing number of dynamic driving tasks have been developed in AD systems (ADSs), such as trajectory planning (Aerts and Schaminée 2017; Chen et al. 2021; Lee and Kum 2020), obstacle avoidance (Cho et al. 2018; Leman et al. 2019; Feng et al. 2020) and lane changing (Zhu et al. 2018; Liu et al. 2022). Yet, many safety-related unknowns need to be investigated toward deploying autonomous vehicles (AVs) with aforementioned dynamic driving tasks. As stated in (Wang et al. 2020), China is the world's largest automotive market and is ambitious for AVs development. Moreover, according to (Chen et al. 2023), "AD accident" is among the top three most-searched keywords in China. Recently, the Beijing Innovation Center for Mobility Intelligent (BICMI) reported the on-road AV testing in the restricted areas in Beijing that by July 2023, the autonomous driving mileage has exceeded 17 million km (BICMI 2023). However, there are few disengagement and accident reports are available along with these testing activities yet, to the best of the authors' knowledge. It would be meaningful if the accident-related information can be available publicly, and the shared information could be beneficial for stakeholders to promote the safety of AVs and build the customers' confidence in AVs. On the other hand, as an illustration in U.S., from July 2021 to May 2022, automakers reported nearly 400 crashes involving vehicles equipped with partially automated driver-assist systems on U.S. roads, including 273, 90 and 10 crashes involving Teslas, Honda and Subaru, respectively, according to statistics released by U.S. safety regulators (Wagner 2022). According to the statistics from the National Highway Traffic Safety Administration (NHTSA) (NHTSA 2022), up to May 2022, there are 132 crashes involving AVs reported officially. In these 132 crashes, 106 crashes reported collisions with other vehicles, and 11 crashes involved vulnerable road users (7 with cyclists, 2 with motorcycles and another 2

with non-motorist electric scooters). NHTSA also stated that collisions between human-driven vehicles (HVs) and AVs are the main type of collisions involving AVs, of which collisions that HVs hit AVs from behind (called HV-AV collisions) make up more than 30% (Petrović et al. 2020; Mohammadian et al. 2021; Wang et al. 2022). Hence, there is a pressing need for effective methods to investigate the risk of HV-AV collisions.

With the aim of understanding human driving intention/behaviour, particularly the brake control, and investigating HV-AV collision risk, when analyzing the existing studies, one can notice that using models to achieve such an aim is gaining popularity. In the existing studies, models are often employed to generate driving behaviours further to achieve dynamic driving tasks (Jeong and Yi 2019; Ma et al. 2022; Tang et al. 2021; Chen et al. 2020; Yoo and Langari 2018; Xia et al. 2021), analyse crash risk (Arbabzadeh and Jafari 2017; Strickland et al. 2018; Muzahid et al. 2020), or respond to warnings and upcoming threats during driving (Bärgman et al. 2017; Markkula 2014; Svärd et al. 2017; Svärd et al. 2021). Since AVs need to share roads with HVs in the near future, some existing models adopt end-to-end approaches based on artificial intelligence algorithms to predict driving responses while ignoring the inherent characteristics of human drivers in reality, which leaves little or no time for other vehicles to react. With this in mind, (Xia et al. 2021) developed a Human-like Lane Changing Intention Understanding Model (HLCIUM) for ADSs to understand the lane changing intentions of surrounding vehicles, which shows efficiency and robustness in complex real urban traffic datasets. To model the interaction between AVs and HVs, (Yoo and Langari 2018) developed a game theory based approach that allows for assessing the time evolution of potential collision paths. In this work, the authors implement a reachability analysis of the solution set of a simple hybrid dynamical system that captures the kinematics of the lane-change process. The scenarios investigated in (Yoo and Langari 2018) appear to produce intuitively reasonable behaviours that seem consistent with ordinary driving behaviours, and highlight the prospects of this approach being implemented in AD strategies. On the other hand, (Arbabzadeh and Jafari 2017) proposed a data-driven approach to quantitatively predict traffic risk that can be customized for individual drivers by including driver-specific variables. The developed predictive

model can be used to support a multitude of applications, including preventing crashes involving vehicles equipped with an ADS or an Advanced Driver Assistance System (ADAS), safety risk profiling of drivers, and safety risk scoring of roadway segments for dynamic hotspot analysis.

Over the last decades, numerous models have been elaborated to describe the driver steering/braking control to respond to warnings and upcoming threats in various traffic situations (Svärd et al. 2021; Markkula et al. 2012), so as to avoid collisions. These models are useful for performing virtual simulations for the purpose of road safety analysis (Bärgman et al. 2017), and can be applied to traffic scenarios with a mix of AVs and regular vehicles. However, most of these models for driver avoidance response simulation are mainly based on the basic kinematics, a scenario-independent distribution of the driver reaction time or predetermined intervention profiles; moreover, they principally adopt an arbitrary assumption that drivers always keep their eyes on the road (Svärd et al. 2021), while the driver's sight is impossible to always fully focus on the road during driving in reality. Yet, some works have figured out that drivers decide their avoidance responses mainly based on visual looming (the optical expansion of the size of a vehicle on the retina (Svärd et al. 2021)), which basically describes how fast the object in front is increasing in size as it is getting closer (Fajen 2008; Markkula et al. 2016). Namely, the actual visual looming is measured as $P_0(t) = \frac{\theta^{'}(t)}{\theta(t)}$, where $\theta(t)$ represents the optical size of the lead vehicle on the retina of the driver of the vehicle behind, reflected by horizontal angle and calculated by $\theta(t) = 2\arctan\frac{W}{2d(t)}$; while $\theta^{'}(t)$ is the expansion rate of the size of the lead vehicle, which can be considered as the stimulus intensity towards the driver of the following vehicle and calculated by $\theta^{'}(t) = -\frac{Wd^{'}(t)}{d(t)^2+\frac{W^2}{4}}$, where W is the width of the lead vehicle, and $d(t)$ denotes the longitudinal distance between the lead vehicle's rear bumper and the following vehicle's front bumper (Markkula 2014; M. et al. 2021). Besides, driver braking control also depends on the sensory impact of primitive motor actions (Markkula et al. 2018; Giszter 2015). In this respect, (Svärd et al. 2017; Svärd et al. 2021) developed visual-looming based models that incorporate the impact of Off-Road-Glance (ORG, see the description in Section 2) and the sensory impact of primitive motor actions, to simulate the driver braking control. Nevertheless, the joint effect of Time-Headway (THW, see the description in Section 2) and ORG on drivers' avoidance

response fails to be considered in the aforementioned models.

Based on the analysis of related works, it is worth noticing that most existing studies for investigating AV-related collision risk have rarely comprehensively taken into account important aspects of human driving intention/experience, vision-based expectancy or inherent characteristics of human driving (e.g., reaction time, ORG, etc.). To tackle the aforementioned issues, in this paper, we proposed a Human-like Brake Control (HLBC) model and use it to investigate the HV-AV rear-end collisions in the Stop-in-Lane (SiL) risky scenario where rear-end collisions are quite likely to occur. Specifically, the unique contributions of the present study are as follows:

1) proposing a Human-like Brake Control (HLBC) model that takes into account human driving intention, vision-based expectancy and certain inherent characteristics of human driving, and can achieve human-like braking based on a dynamic accumulation of braking-needed evidence;
2) originally developing the joint distribution of ORG and THW, which is integrated into the HLBC model framework to simulate the glance distraction of drivers and facilitates the HLBC model emulating the driver braking control in reality;

The remainder of the paper is organized as follows. Section 2 elaborates on the HLBC model framework proposed, and the evaluation of the HLBC model performance. Section 3 is dedicated to the implementation of the HLBC approach in the case study of investigating the HV-AV collision risk in the "SiL" scenario and analyses the outcomes of the case study. Finally, some concluding remarks and future works are given in Section 4.

METHOD

In this section, we will elaborate on the model-based approach proposed to estimate the collision probability via simulation by leveraging the HLBC model and the joint distribution of ORG and THW.

The HLBC model

The proposed HLBC modelling framework consists of four phases, as shown in Fig. 1:

1) Accumulation of evidence: the driver responds according to the accumulated evidence based on looming. The evidence contains two aspects, i.e., supporting the brake control, or against the need of brake control.
2) Tuning magnitude of control adjustments: the driver brakes according to the severity of the situation.
3) Prediction of sensory inputs: the driver makes a prediction of how the control adjustment will affect future sensory inputs. Namely, the driver predicts how the looming will decrease due to each braking action.
4) Control of motor primitives: the driver brakes in steps based on the prediction of sensory inputs. New adjustments based on the combination of ORG and THW are generated to perform more accurate human-like brake control responses.

Several quantities in the HLBC framework are defined as follows.

$P_1(t)$ represents the initial combined perceptual input, which can be defined as follows:

$$P_1(t) = K \cdot E(t) - M, \tag{1}$$

where $E(t)$ denotes the accumulated evidence of looming for or against the need of brake control; K is a free model parameter and corresponds to the weight of the evidence; M is a free model parameter.

$\phi(t)$ is the accumulated looming predictive deviation, and is defined as follows:

$$\phi(t) = \int \{P_0(t) - [P_1(t) + P_2(t) + \delta(t)]\}, \tag{2}$$

where $P_0(t) = \frac{\theta^{'}(t)}{\theta(t)}$ as it is defined in Section 1; $\delta(t)$ denotes the Gaussian zero-mean white noise; $P_2(t)$ represents the looming prediction based on prior braking adjustments. The definition of $P_2(t)$ is given as follows:

$$P_2(t) = \sum_{i=1}^{n} [\phi^{'}(t_i)] H(t - t_i), \tag{3}$$

where n is the number of brake adjustments; t_i corresponds to the time of issuing the i^{th} individual adjustment; $H(t)$ is defined by Eq. (4), shown as follows:

$$H(t)\begin{cases} = 0, & \text{for } t \geq T \\ \rightarrow 1, & \text{for } t \rightarrow 0^{+}, \\ \rightarrow 0, & \text{for } t \rightarrow T^{-} \end{cases} \tag{4}$$

where T is a free model parameter representing the adjustment duration.

$C(t)$ as defined by Eq. (5) is interpreted as the brake signal generated based on successive adjustments.

$$C(t) = \sum_{i=1}^{n} w \cdot P_{O,T}(t_i)\phi^{'}(t_i)G(t - t_i), \tag{5}$$

$P_{O,T}(t_i)$ is the joint distribution of ORG and THW at the instant t_i, which approximates Gamma distribution $\Gamma(t_i)$ according to our preliminary experiment; w is the weight assigned to $P_{O,T}(t_i)$; $G(t)$ is interpreted as the shape of each brake adjustment and is defined as follows:

$$G(t) = \begin{cases} 0, & \text{for } t \leq 0 \\ \\ 1, & \text{for } t \geq T \end{cases}, \tag{6}$$

Note that, as defined by Eq. (6), the further control adjustment $G(t)$ will only affect the brake performed after t_i up until when it is completed.

Joint probability distribution of ORG and THW

ORG emulates the fact that the driver is sometimes looking away from the road, which is an inherent feature of human driving behaviours. The introduction of ORG can make the HLBC model more realistic. On the other hand, THW reflects the distance between the head of the following car and the head of the lead car, which is given as a time quantity. As shown in Figs. 2 and 3, the distributions of ORG and THW are generated respectively, based on real data records from an Original Equipment Manufacturer (OEM), and "Count" is reflected by the histogram representation. One can observe that the ORGs shorter than 1 second occur most frequently, which means short

glances occur more frequently than long ones. Similarly, the trend of the THW histogram reaches a peak at 1.3 seconds, which represents the highest frequency of occurrence within a short time. Sequentially, the ORG and THW variables are adopted jointly to optimize the control action; namely, the joint probability distribution $P_{O,T}(t_i)$ in Eq. (5) is generated and integrated into the HLBC model, as shown in the framework in Fig. 1.

Validation of the model performance

Model fitting

The dataset used for evaluations consists of the naturalistic data from real-world crashes and near-crashes collected in the driving study SHRP2 (SHRP2 2013) (open source), and the real data records from the OEM (confidential source). We finally selected 255 rear-end collisions/near-collisions on public roads from the dataset for model performance evaluation. The drivers involved in the selected events are with relatively equal gender, i.e., about 44% females and 56% males, and the average age of drivers is about 36. The detailed data information is shown in Table 1.

The Particle Swarm Optimization (PSO) algorithm (Clerc and Kennedy 2002; Zhang et al. 2015) is employed to find the optimal parameter values for HLBC model parameter fitting and reduce time-consuming. The PSO algorithm has several parameters that need to be set before running the algorithm. The most important parameters are: **1)** Population size (N), which is the number of particles in the population. We set 4 particles per parameter in our study. **2)** Maximum number of iterations (r), which is the number of times that the algorithm will iterate through the population. The range of r in our study is set as [50, 70]. **3)** Inertia weight (w), which is a weight factor that determines the impact of a particle's velocity on its movement. It should be between 0 and 1. **4)** Cognitive learning rate (c_1), which is a learning rate that determines the particle's movement towards its personal best position. It should be between 0 and 2. **5)** Social learning rate (c_2), which is a learning rate that determines the particle's movement towards the global best position found by its neighbours. It should be between 0 and 2. The initialization ranges and boundaries for the free model parameters of the HLBC model are shown in Table 2.

Model performance evaluation

To evaluate the performance of our HLBC model, we first conducted evaluations to investigate the output longitudinal deceleration, the looming prediction, and the output brake signal of the HLBC model, while considering a rear-end scenario with a lead car issuing a constant brake signal and releasing later. The evaluation results are shown in Fig. 4. In fact, the HLBC model controls a car to perform braking to react to a braking action issued by the lead car when the accumulation of braking evidence is sufficient. The comparison between the HLBC predicted looming and the actual looming reveals that the HLBC model has a sound prediction performance when it comes to simulating human brake control. Besides, the comparison shows that the performance of the HLBC model in terms of looming prediction surpasses that of the relevant model developed in (Svärd et al. 2017) (cf. Figure 2 in (Svärd et al. 2017)).

It is worth mentioning that we also performed Log-likelihood (LL) statistic (Liang et al. 2018) and Pearson Chi-Square (PCS) statistic (Liang et al. 2018) to further evaluate the model performance. The mathematical definitions of LL and PCS are given by Eqs. (7) and (8).

A higher LL value represents a more preferred model. The closer the PCS for Goodness-Of-Fit (GOF) is to the degree of freedom (DF), the better the model fits the data source (Liang et al. 2018; Liang and Ghazel 2023). Here, we calculate p-value to assess how close is the PCS to the corresponding DF. The statistical evaluation results are shown in Table 3. We also evaluated the BWL_{rc} model (a brake model considering looming with reduced complexity) which has the best performance among the relevant models proposed in (Svärd et al. 2021) and is the improved version of the model in (Svärd et al. 2017), by performing fitting through the PSO method with the given inputs of our selected data source, and the comparison between our HLBC model and the BWL_{rc} model is shown in Table 3 as well.

$$\text{LL} = \sum_{i=1}^{n} ln(\hat{C}_i) \tag{7}$$

$$\text{PCS} = \sum_{i=1}^{n} \frac{(\Delta P_i)^2}{\hat{P}_i} \tag{8}$$

where n is the sample size; $\hat{C}_i$ is the estimated braking control action; ΔP_i is the deviation between actual looming and estimated looming, and $\hat{P}_i$ is the estimated looming.

Some findings can be noticed: 1) the t-statistic values of all model parameters are higher than 1.96, which indicates that the confidence level of the model parameter fitting can fulfil 95%; 2) as for the LL value, the HLBIM model is also the preferred one, since the LL value of the HLBIM model is higher than that of the BWL_{rc} model; 3) for the PCS analysis, we set 0.05 as the statistical significance level of GOF and one can notice that the HLBC model have a good GOF with p-value >0.05. These superiorities indicate that the HLBC model can faithfully imitate the driver brake control in reality, which is the base for the following case study.

CASE STUDY

In this section, we will discuss the simulation-based case study while considering the risky scenario of a lead car decelerating to stop in a lane.

Preliminaries

Firstly, the preliminary experimental design for the case study based on a simulation experiment needs to be clarified for the defined scenario, shown as follows:

1) the opponent (following) car is controlled by the HLBC model with reactions based on visual cues generated depending on the lead car braking, to emulate the human control of the braking response of the following vehicle;
2) the lead car is simulated as a High AD (HAD) level vehicle (configured by the OEM's prototype application under development) that can fulfil SAE L4 requirements (SAE 2021);
3) in the scenario considered, the two cars have the same initial speed.

It is worth noticing that, according to (Petrović et al. 2020), an HV hitting an AV from behind is one of the main types of collisions that occur between HVs and AVs while it has been rarely investigated in relevant existing studies. That is why in our study, we consider the scenario where an HV is following an AV.

Case: HAD car decelerating to stop in lane

Purpose

Fig. 5 illustrates the scenario of a HAD car decelerating to stop in a lane with a car-following situation. Specifically, the HAD car is decelerating with a given deceleration level, followed by the opponent car. Meanwhile, the opponent car initiates the braking action (controlled by the HLBC model) depending on the deceleration of the front one. In this case, we investigate the probability of HV-AV collision occurrence in the SiL scenario by considering various collision speeds (the instantaneous relative speed of the two cars at the exact moment when they right collide with each other), initial speeds, decelerations of the opponent car and decelerations of the HAD car, respectively.

Assumptions

In order to facilitate the simulation, several assumptions have been considered for this case, as listed below:

> **Assumption 1:** the deceleration of the opponent car shall fulfil: $|a_{Opponent}| < 1g$, where g represents the gravitational acceleration (according to the industrial experience, the maximum car deceleration shall be less than $1g$).
>
> **Assumption 2:** the deceleration of the HAD car shall fulfil: $|a_{HAD}| < 1g$.
>
> **Assumption 3:** the THW between the opponent car and the HAD car shall fulfil: $THW \leq$ 5.5 s (according to the statistical analysis in Fig. 3, the probability of the THW duration longer than 5.5 s is almost zero). Indeed, a bigger THW value reflects a too long distance separating the two cars, so the driver of the following car is unlikely to trigger a brake as he/she is far from the lead car.

Results and discussion

In Fig. 6, we show a detailed analysis of the probability of collision according to different collision speeds, initial speeds and decelerations of the opponent and HAD cars, respectively, through twelve charts (sub-figures). In the subsequent part, we will use "R_C_" to define the ID

of sub-figures, e.g., R1C2 represents the plot located in the 1st row and 2nd column. Besides, rows reflect the impact of increasing brake capability of the opponent car on the probability of collision by considering different deceleration intensities of the HAD car; while columns reflect the impact of increasing collision speed on the probability of collision by considering different deceleration intensities of the HAD car. Additionally, the X-axis represents the same initial speed of both cars (see Section 3), the Y-axis represents the probability of collision.

As illustrated in Fig. 6, taking the plot R2C3 for instance, the black dashed line shows that there is 9% probability of collision with collision speeds over 50 km/h if both vehicles travel at an initial speed of 70 km/h and the HAD vehicle is braking at a deceleration of $0.4g$, while the opponent car behind brakes with a maximum deceleration of $0.7g$. In the plot R1C3 (the opponent car behind is braking at $0.5g$ maximum instead of $0.7g$ in the plot R2C3), the black dashed line shows that the probability of collision soars from 9% to 43% at an initial speed of 70 km/h, compared with that in the plot R2C3. Further, as shown in the plot R2C4 (the collision speed is $\geq$70 km/h instead of $\geq$50 km/h in the plot R2C3), the black dashed line shows that the probability of collision decreases from 9% to 1% at an initial speed of 70 km/h, compared with that in the plot R2C3. One can notice that the collision probability goes down at a relatively high collision speed, compared with the probability of collision at a lower collision speed. The potential reason could be that the collision speed is ultimately depending on the combination of ORG and THW distributions that less likely leads to a high collision speed as time goes on (see Figs. 2 and 3). Moreover, all the sub-figures indicate that regarding the impact of the initial speed, the probability of collision always raises as the initial speed increases. For example, the black dashed line in the plot R2C3 shows that the probability of collision goes up from 9% to 82% as the initial speed increases from 70 km/h to 90 km/h illustrated by the X-axis values.

Actually, through the figures above, one can explore the underlying perspective of mechanism/reasoning behind HVs rear-ending AVs that the existing AD systems often utilize end-to-end ML methods for making brake decisions without adequately considering the coupling effects of various heterogeneous factors such as driver intention/experience, inherent characteristics of hu-

man driving, and vision-based expectancy, which leads to inaccuracies in the timing and magnitude of collision avoidance control actions. Particularly, these systems often produce single and heavy braking actions (such as hard braking), which are ineffective in achieving smooth dynamic collision avoidance. This can result in surrounding vehicles having almost no time to react appropriately in emergency situations, especially during car-following scenarios, thereby increasing the risk of rear-end collisions.

CONCLUSIONS

In the present paper, we have developed a model called HLBC to emulate human drivers' braking control, for the purpose of investigating the relation between collision occurrence and various factors in the risky scenario "Stop-in-Lane". The parameters considered in our study are respectively: collision speeds, initial speeds and decelerations of cars under test.

The main contributions of our study are as follows:

1) The HLBC model is proposed to emulate the driver braking control. It takes into account deceleration/braking intention and experience of human driving (such as a dynamic, mild and stepping brake), vision-based expectancy and certain inherent characteristics of human driving, e.g. ORG, and achieves human-like braking based on a dynamic accumulation of braking-needed evidence. In addition, the HLBC model can be also applied to other scenarios relevant to vehicle braking response.
2) The joint distribution of ORG and THW is integrated into the HLBC model framework to emulate the glance distraction of drivers when they perform dynamic vehicle control, which facilitates the HLBC model faithfully imitating the driver brake control in reality.

To sum up, the HLBC model has a sound prediction performance when it comes to simulating human brake control, which is attested by the results of the model performance validation. Moreover, the findings of the case study give a profound perspective on the dynamic driving conditions that have a significant impact on collision occurrence in the "Stop-in-Lane" scenario. In addition, the present study can provide the guidance for designing a new type of human-like AD systems. The

reason for developing human-like AD systems is that by integrating human driving experience for decision-making and understanding the behavior and intentions of surrounding traffic participants in the same way as human drivers doing, the human-like AD system can improve its own decision-making capability, enhance the acceptability of AVs from the public, and promote eco-driving. In future work, we will introduce Neural Networks, to improve the looming prediction of the HLBC model. Besides, more risky scenarios (e.g., car following during city rush hour congestion, cut in, and merging onto/separating from the freeway) will be investigated by using the HLBC model for the purpose of improving AD safety. Additionally, it is necessary to comprehensively assess its functional safety (ISO26262 2018) and Safety Of The Intended Functionality (SOTIF) (ISO21448 2022) when it is going to be embedded in AVs for commercial production.

ACKNOWLEDGEMENTS

This study was supported by Heilongjiang Provincial Natural Science Foundation of China "LH2023E055", and the Fundamental Research Funds for the Central Universities (Science and technology leading talent team project) "2022JBXT003".

DATA AVAILABILITY STATEMENT

Some or all data, models, or code generated or used during the study are proprietary or confidential in nature and may only be provided with restrictions.

REFERENCES

Aerts, H. and Schaminée, H. (2017). "How software is changing the automotive landscape." *IEEE Software*, 34(6), 7–12.

Arbabzadeh, N. and Jafari, M. (2017). "A data-driven approach for driving safety risk prediction using driver behavior and roadway information data." *IEEE Transactions on Intelligent Transportation Systems*, 19(2), 446–460.

Bärgman, J., Boda, C., and Dozza, M. (2017). "Counterfactual simulations applied to shrp2 crashes: The effect of driver behav-ior models on safety benefit estimations of intelligent safety systems." *Accident Analysis and Prevention*, 102, 165–180.

BICMI (2023). "Beijing autonomous vehicle road test report." *Report no.*, Beijing Innovation Center for Mobility Intelligent, <http://www.mzone.site/>.

Chen, J., She, R., Yang, S., and Ma, J. (2023). "The city scale effect and the baidu index prediction model of public perceptions of the risks associated with autonomous driving technology." *International Conference on Human-Computer Interaction*, 425–441.

Chen, J., Zhang, C., Luo, J., Xie, J., and Wan, Y. (2020). "Driving maneuvers prediction based autonomous driving control by deep monte carlo tree search." *IEEE Transactions on Vehicular Technology*, 69(7), 7146–7158.

Chen, Z., Wang, S., Yu, B., Liang, H., Li, B., and Zheng, X. (2021). "A robust trajectory planning method based on historical information for autono-mous vehicles." *5th International Conference on Robotics and Automation Sciences (ICRAS)*, 198–205.

Cho, J., Pae, D., Lim, M., and Kang, T. (2018). "A real-time obstacle avoidance method for autonomous vehicles using an obstacle-dependent gaussian potential field." *Journal of Advanced Transportation*, 2018, 1–15.

Clerc, M. and Kennedy, J. (2002). "The particle swarm-explosion, stability, and convergence in a multidimensional complex space." *IEEE Transactions on Evolutionary Computation*, 6(1), 58–73.

Fajen, B. (2008). "Perceptual learning and the visual control of braking." *Perception & Psychophysics*, 70(6), 1117–1129.

Feng, P., Zou, J., Li, H., and Gao, S. (2020). "An obstacle avoidance method for autonomous vehicle in straight road based on expanded circle." *2020 Asia-Pacific Conference on Image Processing, Electronics and Computers (IPEC)*, 43–46.

Giszter, S. F. (2015). "Motor primitives—new data and future questions." *Current Opinion in Neurobiology*, 33, 156–165.

ISO21448 (2022). "Road vehicles - safety of the intended functionality (E).

ISO26262 (2018). "Road vehicles - functional safety (E), 2nd edition.

Jeong, Y. and Yi, K. (2019). "Target vehicle motion prediction-based motion planning frame-

work for autono-mous driving in uncontrolled intersections." *IEEE Transactions on Intelligent Transportation Systems*, 22(1), 168–177.

Lee, K. and Kum, D. (2020). "Longitudinal and lateral integrated safe trajectory planning of autonomous vehicle via friction limit." *20th International Conference on Control, Automation and Systems (ICCAS)*, 1177–1180.

Leman, Z., Ariff, M., Zamzuri, H., Rahman, M., and Mazlan, S. (2019). "Model predictive controller for path tracking and obstacle avoidance manoeuvre on autonomous vehicle." *12th Asian Control Conference (ASCC)*, 1271–1276.

Liang, C. and Ghazel, M. (2023). *LaTeX: Accident prediction modeling approaches for European railway level crossing safety*. IntechOpen Limited DOI: 10.5772/intechopen.109865.

Liang, C., Ghazel, M., Cazier, O., and El-Koursi, E. (2018). "Developing accident prediction model for railway level crossings." *Safety science*, 101, 48–59.

Liu, Y., Zhou, B., Wang, X., Li, L., Cheng, S., Chen, Z., Li, G., and Zhang, L. (2022). "Dynamic lane-changing trajectory planning for autonomous vehicles based on discrete global trajectory." *IEEE Transactions on Intelligent Transportation Systems*, 23(7), 8513–8527.

M., S., Bärgman, J., and Victor, T. (2021). "Detection and response to critical lead vehicle deceleration events with peripheral vision: Glance response times are independent of visual eccentricity." *Accident Analysis and Prevention*, 150, 105853.

Ma, C., Xue, J., Liu, Y., Yang, J., Li, Y., and Zheng, N. (2022). "Data-driven state-increment statistical model and its application in autonomous driving." *IEEE Transactions on Intelligent Transportation Systems*, 19(12), 3872–3882.

Markkula, G. (2014). "Modeling driver control behavior in both routine and near-accident driving." *The human factors and ergonomics society annual meeting*, 58(1), 879–883.

Markkula, G., Benderius, O., Wolff, K., and Wahde, M. (2012). "A review of near-collision driver behavior models." *Human factors*, 54(6), 1117–1143.

Markkula, G., Boer, E., Romano, R., and Merat, N. (2018). "Sustained sensorimotor control as intermittent decisions about prediction errors: Computational framework and application to

ground vehicle steering." *Biological cybernetics*, 112, 181–207.

Markkula, G., Engström, J., Lodin, J., Bärgman, J., and Victor, T. (2016). "A farewell to brake reaction times? kinematics-dependent brake response in natu-ralistic rear-end emergencies." *Accident Analysis and Prevention*, 95, 209–226.

Mohammadian, S., Haque, M., Zheng, Z., and Bhaskar, A. (2021). "Integrating safety into the fundamental relations of freeway traffic flows: A con-flict-based safety assessment framework." *Analytic methods in accident research*, 32, 100187.

Muzahid, A., Kamarulzaman, S., and Rahim, M. (2020). "Learning-based conceptual framework for threat assessment of multiple vehicle collision in autonomous driving." *Emerging Technology in Computing, Communication and Electronics (ETCCE)*, 1–6.

NHTSA (2022). "Summary report: Standing general order on crash reporting for automated driving systems." *Report No. DOT HS 813 324*, National Highway Traffic Safety Administration.

Petrović, D., Mijailović, R., and Pešić, D. (2020). "Traffic accidents with autonomous vehicles: type of collisions, manoeuvres and errors of conventional vehicles' drivers." *Transportation Research Procedia*, 45, 161–168.

SAE (2021). "Taxonomy and definitions for terms related to driving automation systems for on-road motor vehicles." *Report No. SAE J3016_202104*, SAE International.

SHRP2 (2013). "The 2nd strategic highway research program naturalistic driving study dataset." *Report no.*, Transportation Research Board of the National Academy of Sciences, <http://www.mzone.site/>.

Strickland, M., Fainekos, G., and Amor, H. (2018). "Deep predictive models for collision risk assessment in autonomous driving." *2018 IEEE International Conference on Robotics and Automation (ICRA)*, 4685–4692.

Svärd, M., Markkula, G., Bärgman, J., and Victor, T. (2021). "Computational modeling of driver pre-crash brake response, with and without off-road glances: Parameterization using real-world crashes and near-crashes." *Accident Analysis and Prevention*, 163, 106433.

Svärd, M., Markkula, G., Engström, J., Granum, F., and Bärgman, J. (2017). "A quantitative driver

model of pre-crash brake onset and control." *The human factors and ergonomics society annual meeting*, 61(1), 339–343.

Tang, T., Gui, Y., and Zhang, J. (2021). "Atac-based car-following model for level 3 autonomous driving considering driver's acceptance." *IEEE Transactions on Intelligent Transportation Systems*, 23(8), 10309–10321.

Wagner, O. (2022). "Nearly 400 car crashes in 11 months involved automated tech, companies tell reg-ulators." *Report no.*, NPR news, <https://www.npr.org/2022/06/15/1105252793/nearly-400-car-crashes-in-11-months-involved-automated-tech-companies-tell-regul>.

Wang, C., Chen, F., Zhang, Y., Wang, S., Yu, B., and Cheng, J. (2022). "Temporal stability of factors affecting injury severity in rear-end and non-rear-end crashes: A random parameter approach with heterogeneity in means and variances." *Analytic methods in accident research*, 35, 100219.

Wang, K., Li, G., Chen, J., Long, Y., Chen, T., Chen, L., and Xia, Q. (2020). "The adaptability and challenges of autonomous vehicles to pedestrians in urban china." *Accident Analysis and Prevention*, 145, 105692.

Xia, Y., Qu, Z., Sun, Z., and Li, Z. (2021). "A human-like model to understand surrounding vehicles' lane changing intentions for autonomous driving." *IEEE Transactions on Vehicular Technology*, 70(5), 4178–4189.

Yoo, J. and Langari, R. (2018). "A predictive perception model and control strategy for collision-free autonomous driving." *IEEE transactions on intelligent transportation systems*, 20(11), 4078–4091.

Zhang, Y., Wang, S., and Ji, G. (2015). "A comprehensive survey on particle swarm optimization algorithm and its applications." *Mathematical problems in engineering 2015*, 20(11), 1–38.

Zhu, B., Yan, S., Zhao, J., and Deng, W. (2018). "Personalized lane-change assistance system with driver behavior identification." *IEEE Transactions on Vehicular Technology*, 67(11), 10293–10306.

List of Tables

TABLE 1. Data information

Data categories	Total events	Rear-end collisions	Near-collisions
Quantity	255	93	162
Data source	OEM data 65.9% SHRP2 data 34.1%	OEM data 64.5% SHRP2 data 35.5%	OEM data 66.7% SHRP2 data 33.3%
Driver gender	Male 56.1% Female 43.9%	Male 58.1% Female 41.9%	Male 54.9% Female 45.1%
Driver age	< 30 21.3% 30-39 36.4% 40-49 24.2% 50-59 18.1%	< 30 26.9% 30-39 33.3% 40-49 25.8% 50-59 14.0%	< 30 17.9% 30-39 38.3% 40-49 23.5% 50-59 20.4%

TABLE 2. Initialization ranges of free model parameters

Free parameters	N	r	w	c_1	c_2	K	M	ϕ_0	T_{G0}	T_{G1}
Initialization range	[4, 40]	[50, 70]	[0, 1]	[0, 2]	[0, 2]	[1, 40]	[0, 10]	[0, 1]	[0.5, 4]	[0.5, 5]

TABLE 3. Parameter values and evaluation results.

Free parameters	N	r	w	c_1	c_2	K	M	ϕ_0	T_{G0}	T_{G1}	LL	PCS
HLBC	4	70	0.36	2	1.49	5.15	3.73	0.91	1.23	2.71	-53.77	73.11 (p-value=0.28)
t-statistic	NA	NA	NA	NA	NA	2.11	3.12	4.54	4.16	6.31	NA	NA
BWL_{rc}	4	70	0.33	2	1.49	NA	NA	NA	NA	NA	-61.06	80.13 (p-value=0.12)

NA means "Not Applicable" since t-statistic is not applicable to PSO inherent parameters, LL and PCS; additionally, the parameters of the BWL_{rc} model are different from those of the HLBIM model.
t-statistic >1.96 corresponds to a 95% confidence level

List of Figures

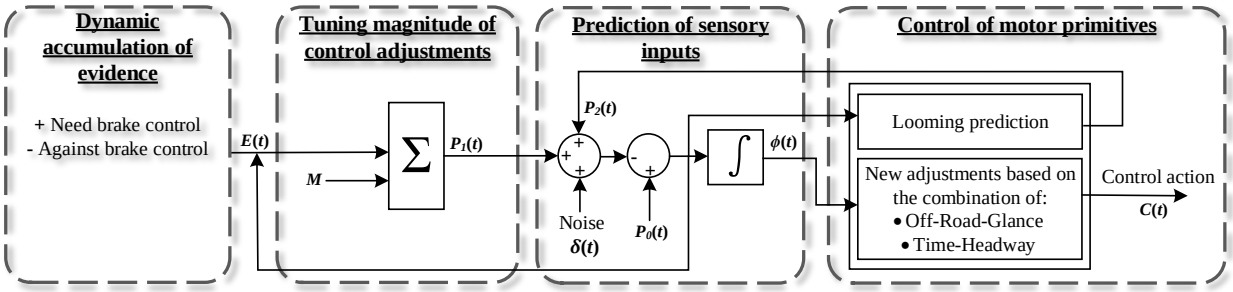

Fig. 1. The modelling framework of HLBC.

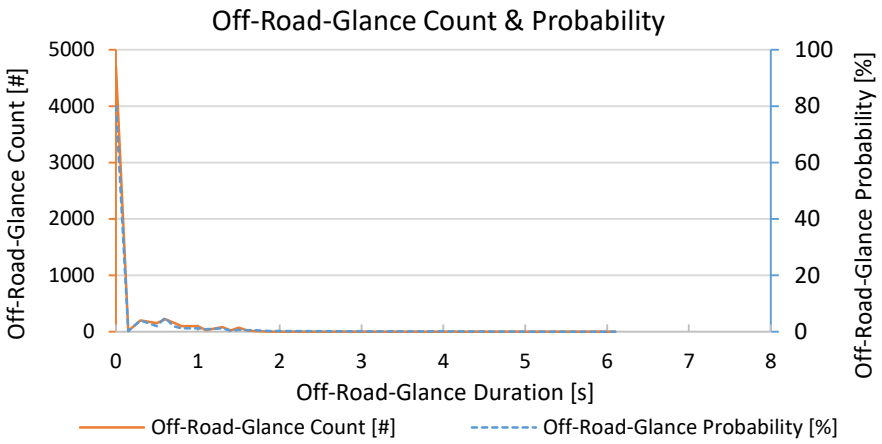

Fig. 2. The histogram and probability of ORG.

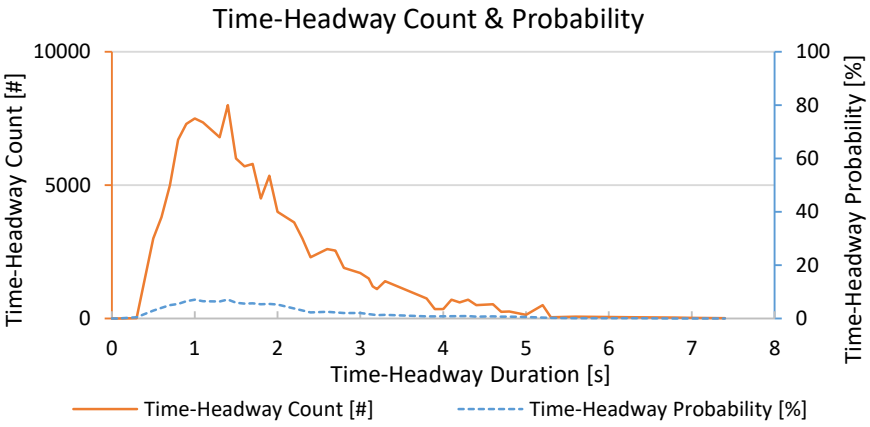

Fig. 3. The histogram and probability of THW.

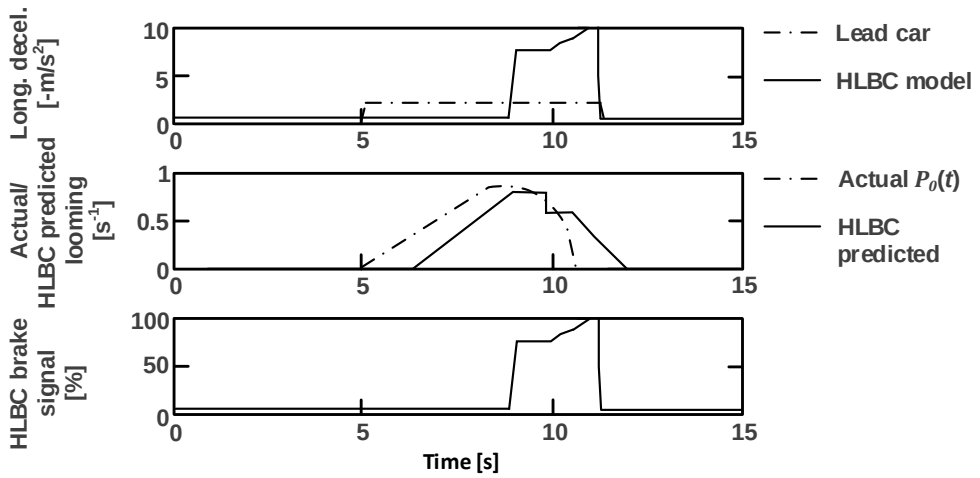

Fig. 4. The performance of the HLBC model and comparison with reality: "Long. decel." represents longitudinal deceleration; the deceleration of the lead car is $0.2g$ (g is the gravitational acceleration); the brake onset of the following car controlled by the HLBC model is at t = 8.5 s.

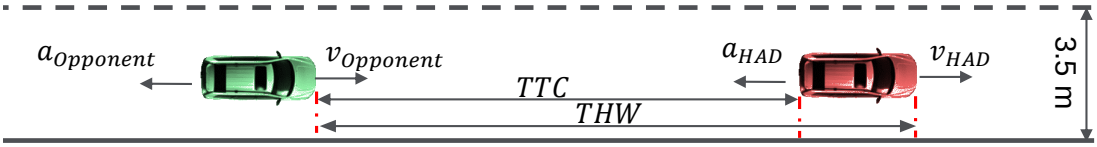

Fig. 5. The scenario illustration: TTC represents Time-To-Collision and the lane width is 3.5 m.

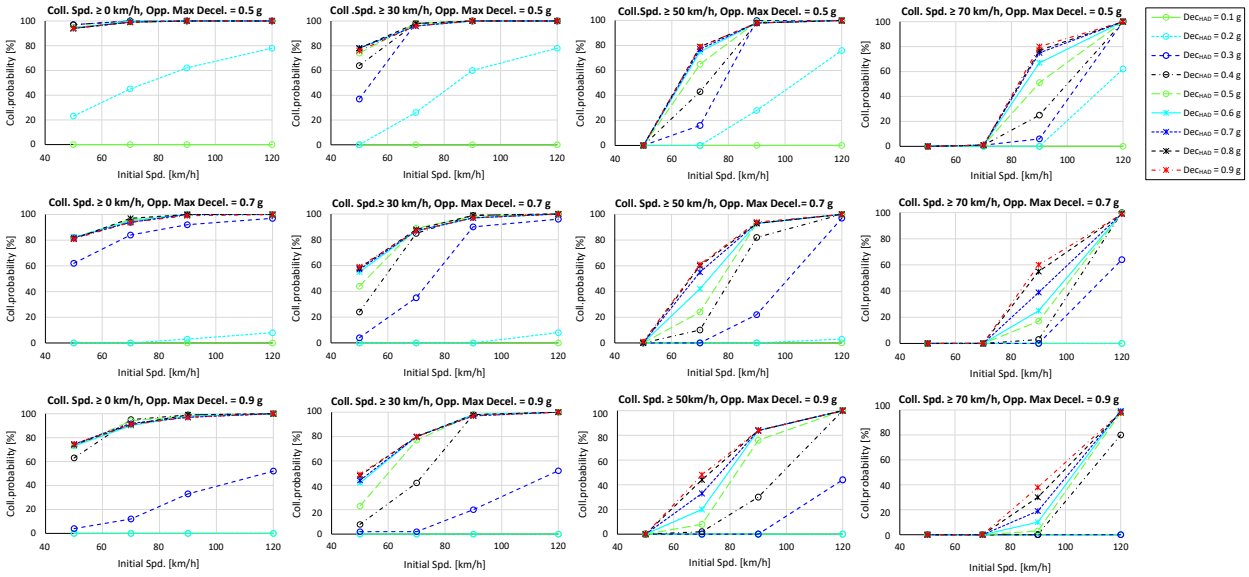

Fig. 6. The probability of collision according to different collision speeds, initial speeds and decelerations of the opponent and HAD cars, respectively.